

Flyback Topology TEM Bipolar Pulse Transmitter

Yong-shou Yang*, Guo-fu Wang, Jin-cai Ye

¹Guilin University of Electronic Technology (GUET), Guilin 541004, China

*Corresponding author, e-mail: ilouis@163.com

Abstract

In the fields of transient electromagnetic (TEM) geophysical exploration, it is necessary to create a bipolar pulse current source with decline edge of high linearity, short turn-off time and high stability. In order to improve detection equipment's practicality, it's urgently needed to miniaturize and improve the reliability of the detection equipment. In this paper, a clamp and prompt drop bipolar pulse current circuit based on Flyback topology is represented, which can accelerate the decline of load current by clamping the coil load with fixed high voltage in the period of current declining. Also, because of this circuit's low power consumption and significantly improvement of the transmitter's energy utilization, chassis's cooling equipment can be greatly reduced and it's easier to miniaturize the transmitter. To start with, the principle of this circuit is represented. Then, the method is given to select the optimal values of circuit's components. Finally, the results of simulation proves the proposed circuit meeting the requirements much better than those reported, with shorter turn-off time, higher linearity, less energy consumption. In general, this circuit has been successfully applied to a new type of detection equipment.

Keywords: turn-off time, pulse current supply, full bridge converter, electromagnetic transmittal

Copyright © 2013 Universitas Ahmad Dahlan. All rights reserved.

1. Introduction

There are many different types of bipolar pulse current supplies and they are also widely used. In the field of electromagnetic detection, electroplating, motor drive, the requirements for the use of pulsed current source with high dynamic response, high stability and high di/dt [1]. For example, transient electromagnetic (TEM) method is a kind of geophysical methods. From the point of the frequency-domain electromagnetic method, the high-frequency component has proved to be favorable to shallow exploration. Ideal step-wave having a continuous spectrum, rich in high frequency components, the ramp step-wave contains fewer high frequency components [2]. Theoretically, if the ideal step-wave is used as transmittal current, geological information of a wide range of stratum, from the surface to several kilometers deep underground, can be detected. Therefore, bipolar pulse current supply, with high linearity of the falling edge, short turn-off delay (the time current dropping to zero) and no current overshoot, is required by transient electromagnetic method in order to make the transmitted waveform approximate to the ideal step-wave. However, due to large load inductance coil, large transmittal current, slow electronic switching speed and electronic components heat loss, some deficiencies exist in electromagnetic transmitter circuits [3]. They are long turn-off delay, uncontrollable falling edge waveform, big whole thermal loss and inconsistent positive and negative pulse. Turn-off delay: turn-off delay means the time transmittal current dropping from the stable value to zero. In this period of time, the primary field does not completely subside, secondary field has been generated. The aliasing causes a serious distortion of the initial response signal. Consequently, the shallow geological information is lost [4]. Therefore, transmit waveform with very short turn-off delay is required in TEM; the absolute value of the current decreasing ratio is required greater than $3 \times 10^4 \text{ A/s}$ usually.

Reference [5-7] proposed trapezoidal pulse circuit. It's a new circuit that realizes energy feedback and accelerates the formation of a stable field by shaping the rising edge of the transmittal current. It also discussed the possibility of electromagnetic transmittal using half-bridge circuit. Reference [8-9] proposed two pulse circuits clamping with fixed voltage. Those circuits accelerate transmittal current's slope of decline, shorten turn-off delay further by using the principle of fixed high voltage clamping. Those circuits briefly introduced above are insufficient: improved RCD, IEDD and quasi-resonant pulse circuits' turn-off delay and current linearity are closely related to load inductor and supply voltage; constant voltage clamp circuit

(CVCC) and enhanced constant voltage clamp circuit (ECVCC) have large heat loss in the part of energy feedback. In other words, they efficiency of energy utilization is low.

To solve the above electromagnetic transmittal problems, the paper proposes a new clamp pulse circuit based on Flyback method (FCVCC). Simulation and experiment has proved that this circuit has good response and energy efficiency.

2. Principle Analysis of Flyback Constant Voltage Clamp Circuit

The inductor current-voltage characteristic of the following equation exists: $L di / dt = u$. It is clear that, for a specific inductance of the load L , in order to speed up the decline of the transmittal current it is necessary to correspondingly increase the voltage u across the load. The BUCK topology of switching power supply is used to produce a fixed high voltage in the literature [1]. Then that fixed high voltage is used to clamp the coil voltage during the current-off period and the current's falling edge waveform is very good. Author is inspired from that, if the Flyback topology of switching power supply is used to complete energy feedback and control the clamping voltage in the TEM transmittal circuit, it can guarantee the transmittal current's short turn-off delay and high linearity during current-off period. Further more, the transmittal circuit's energy utilization can be improved, the transmitter enclosure cooling equipment and space can be saved. Therefore, the new circuit is referred to as Flyback constant voltage clamp circuit (FCVCC). The new Circuit's schematic diagram is shown in Figure 1.

In Figure 1, switches M1, M2, M3, M4 and fast recovery diode D1, D2, D3, D4 form a full bridge circuit. The inductor L1 stands for the self-inductance of the transmittal coil and the resistor R1 is the internal resistance of the coil. The capacitor C1 is the inputs of the constant voltage supply and the diodes D8, D9 clamp the voltage of coil. The pulse transformer TX1, diode D6, capacitor C2 and the switch M5 constitute a discharge circuit of the capacitor C1. The voltage regulator V2, the voltage comparators U1, U2, and the pulse generator V3 constitute a voltage mode PWM circuit.

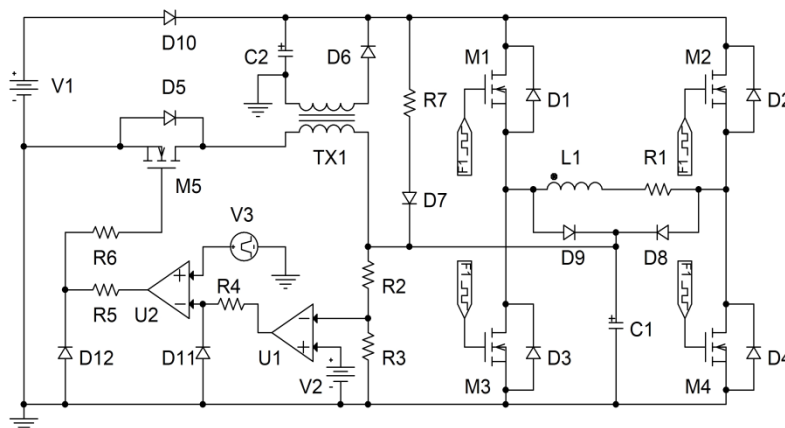


Figure 1. Flyback Constant Voltage Clamp Circuit (FCVCC)

A transmittal cycle can usually be divided into four stages: transmitting a forward pulse current, no current, transmitting a negative pulse current and no current. And four stage's time lengths are all a quarter of the transmittal period. When positive pulse current is transmitted, the switches M1, M4 are on, switches M2, M3 are off; when negative pulse current is transmitted, switches M2, M3 are on, switches M1, M4 are off; when no transmittal current, all four switches M1, M2, M3, M4 are off. Load L1 generates a large induced voltage immediately after all four switches are off, charges capacitor C1 through clamping diodes D8 (positive off) or D9 (negative off).

C1 and discharge-circuit actually constitute a Flyback circuit. As C1 is inputs, C2 is outputs. The new Flyback circuit, which is quite different from conventional Flyback circuit where the outputs voltages are stabilized, stabilizes the inputs voltage by the switching control circuit

and keeps it constant. When C1 voltage is higher than the set value U_{SET} (determined by the voltage reference V2 and the voltage dividing resistors R5, R6), the comparator U1's output turns from high to low. The negative input of comparator U2 has the same voltage with U1's output; the positive input of U2 is connected to the 200 kHz pulse voltage generator V3, so U2 has same output with V3. The pulse voltage output is used for the gate control signal of switch M6 after being clamped by R5 and D12. C1 begins to charge the capacitor C2 through the pulse transformer TX1 and switch M6. When the C1 voltage is less than the set value U_{C1} , U1 output is high and U2 low. The switch M6 is always off. The control waveform above is shown in Figure 2.

The switch control method of Flyback circuit is referred to as gate-control PWM whose operating frequency and pulse width are fixed. Compared with the variable pulse width PWM, the gate-control PWM can output zero pulse in one pulse cycle; compared with the comparator control PWM, the gate-control PWM will not break the MOSFET switch M6 as M6 will not be turned on for a long time continuously and not become very hot; compared with hysteretic control PWM, gate-control PWM circuit is simpler, easier to implement, and less heat loss.

When switches M1, M4 are on, a positive pulse current is transmitted, when switches M1, M4 is off, the positive current begins to decrease. In the following paragraphs, Flyback circuit is analyzed from the time point of M1, M4 are turned off.

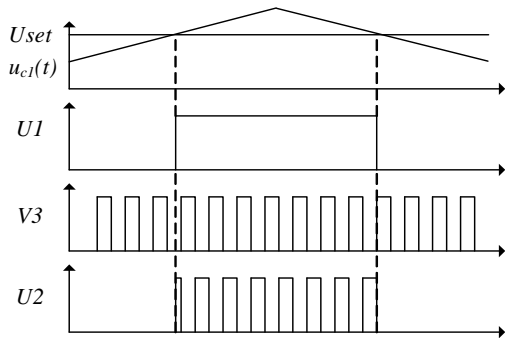


Figure 2. Gate-control PWM Waveform

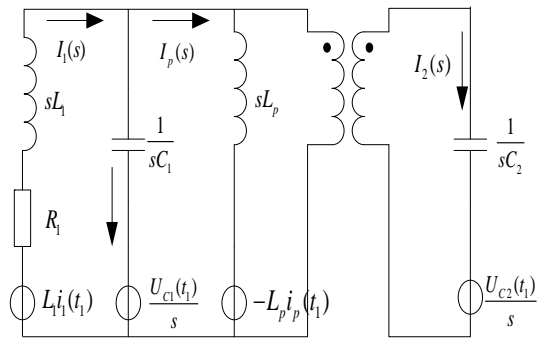


Figure 3. Flyback Circuit's Complex Frequency Domain Model in Second Stage

(1) Stage 1: after the positive switches are turned off, an induced electromotive force generates on the load L1, the induced current $i(t)$ charges C1 through the loop of L1, D8, C1, M3, and parasitic diode D4, so the C1 terminal voltage $U_{C1}(t)$ rise. Because the voltage $U_{C1}(t)$ is less than the setting value U_{SET} , the comparators U1 output is high, U2 output is low, switch M5 is off. Circuit's complex frequency domain expression is shown in Equation (1):

$$U_{C1}(s) = \frac{L_1 i(t_0) - U_{C1}(t_0) / s}{s^2 L_1 C_1 + s R_1 C_1 + 1} + \frac{U_{C1}(t_0)}{s} \tag{1}$$

In the (1), $U_{C1}(t_0)$ denotes the initial voltage on the capacitor C1; $i(t_0)$ denotes the initial current of the inductor L1, i.e. instantaneous load current before turn-off time point.

(2) Stage 2: When the C1 voltage is greater than the setting value U_{SET} , U1 outputs low level, U2 outputs pulse-wave to control the switch M5. C1 charges C2 through the loop of TX1, D6, C2 and M5 in order to keep C1 voltage fixed. Circuit's complex frequency domain model is shown in Figure 3. Complex frequency domain expression:

$$(sL_1 + R_1)I_1(s) - L_1 i_1(t_1) + \frac{U_{C1}(t_1)}{s} + \frac{I_1(s) - I_p(s)}{sC_1} = 0 \tag{2}$$

$$\frac{U_{C1}(t_1)}{s} + \frac{I_1(s) - I_p(s)}{sC_1} - sL_p I_p(s) + L_p i_p(t_1) = 0 \quad (3)$$

$$\frac{1}{n} [sL_p I_p(s) - L_p i_p(t_1)] - \frac{I_2(s)}{sC_2} - \frac{U_{C2}(t_1)}{s} = 0 \quad (4)$$

In the Equation (3) and Equation (4), the $U_{C1}(t_1)$, $U_{C2}(t_1)$ denote respectively the C1, C2 voltage at t_1 moment; n : 1 denotes turns ratio of the pulse transformer TX1; $I_1(t_1)$, $I_2(t_1)$ denote respectively the L1, L2 current at t_1 moment.

(3) Stage 3: The negative switches M2, M3 are off, and the load L1 generates an induced electromotive force. The induced current $i(t)$ charge up C1 along the loop of D9, C1, M4's parasitic diode D5. Circuit's operating principle in negative turn-off period is same as positive turn-off period, and there is no need to repeat that.

After capacitor C2 is charged at the beginning, its voltage is much greater than the supply voltage, so it can significantly accelerate the climb of the load current. Thus, C2 is referred to as the boost capacitor. The resistor R7, diode D7 have protective effect to switch M1, when the positive switch M1 turn instantaneous on, a charging current may pass through the loop of power supply V1, switch M1, diode D9, capacitor C1. The instantaneous charging current is large, and it could burn the switch M1 easily. Because of the protection of the resistor R7 and diode D7, the power supply V1 will charge the C1 to supply voltage before the switch M1 is turned on.

3. Design of Flyback Constant Voltage Clamp Circuit

Known parameters are determined by the designer according to the user's needs and the characteristics of the circuit. The known parameters including: input voltage $U_{in} = 600V$, the output voltage $U_{out} = 260V$, output power P_{out} , efficiency $\eta = 0.9$, switching frequency $f_s = 200kHz$ (or switching period $T = 5\mu s$), the withstand voltage of main switch MOSFET $U_{mos} = 800V$.

3.1. Estimate the Load's Self-inductance and Internal Resistance [10]

The approximation formula of calculating the circular cross-section square coil's self-inductance is shown in Equation (5):

$$L = \frac{\mu_0 a}{\pi} [2 \ln(\frac{2a}{r}) - 3 + \frac{\mu_r}{2}] \quad (5)$$

In Equation (5), a denotes the square coil's side length; μ_0 is the vacuum magnetic permeability ($4\pi \times 10^{-7}H/m$), and r is the wire radius; μ_r means the relative magnetic permeability. The coil used in the actual is a single turn square copper conductors with a cross-sectional area of $10mm^2$ and a side length of $500M$. To replace the parameters in Equation (8) with $a = 500M$, $\pi r^2 = 10 \times 10^{-6}m^2$, $\mu_r = 1$, $\mu_0 = 4\pi \times 10^{-7}H/m$, then get the calculation result is load inductance $L1 = 4.8mH$. The calculation formula of internal resistance is $R = \rho/l/s$; ρ is the resistivity of copper and equals $0.0175\Omega \cdot mm^2/m$ ($20^\circ C$); $l = 2000M$ and $s = 10mm^2$. The calculation result is $R1 = 3.5\Omega$.

3.2. Calculate the Turn-off Delay [1]

Suppose C1 voltage as a constant U_{SET} during the current turn-off period. The calculation formula of turn-off delay is shown in Equation (6):

$$t_d = -\frac{L_1}{R_1} \left[\ln \frac{U_{SET}}{U_{C1} + i(t_0)R_1} \right] \quad (6)$$

In Equation (6), U_{SET} is the stable voltage value $600V$ of capacitor C1; $i(t_0)$ denotes the transmittal current value $30A$; $L1$ stands for self-inductance $4.8mH$ of the transmittal coil; $R1$ is the resistance 3.5Ω of transmittal coil. The calculation result is $t_d = 221\mu s$.

3.3. Calculate the Capacitances of C1 and C2

To the capacitor C1, the lower limit capacitance can be calculated when C1 absorbs just all the coil energy during the current-off period. The capacitance value of C1 can be conditioned using the following Equation (7):

$$\frac{1}{2}L_1I_1^2 - \frac{1}{3}t_dR_1I_1^2 < \frac{1}{2}C_1(U_{C_1}^2(\max) - U_{C_1}^2(\min)) \quad (7)$$

In Equation (7), I_1 denotes the transmittal current value; $U_{C_1}(\max)$ stands for the desired upper limit of C1 voltage fluctuation. The left side of Equation (7) means coil residual energy minus the consumption of the coil resistance (current falling edge is seen as saw tooth approximately). To replace the parameters in Equation (7) with $L_1 = 4.8\text{mH}$, $U_{\text{SET}} = 600\text{V}$, $U_{C_1}(\max) = 610\text{V}$, $I_1 = 30\text{A}$, $R_1 = 3.5\Omega$, $t_d = 221\mu\text{s}$. The calculation result is $C_1 > 318\mu\text{F}$. In the actual circuit, C1 is determined to a $330\mu\text{F}$ aluminum electrolytic capacitor with a withstand voltage 1000V . The C2 capacitance can be calculated with the same method, but the expression is slightly different from above and shown in Equation (8):

$$\frac{1}{2}C_2[U_{C_2}^2(\max) - U_{C_2}^2(t_0)] > \frac{1}{2}L_1I_1^2 - \frac{1}{3}t_dR_1I_1^2 \quad (8)$$

In Equation (8), $U_{C_2}(\max)$ is the desired upper limit of the C2 voltage; $U_{C_2}(t_0)$ stands for the starting voltage of C2 at t_0 moment, and it approximately equals the supply voltage U_{V_1} . To replace the parameters in Equation (8) with $L_1 = 4.8\text{mH}$, $U_{C_2}(\max) = 260\text{V}$, $U_{C_2}(t_0) = 150\text{V}$, $I_1 = 30\text{A}$, then get calculation result: $C_2 > 85\mu\text{F}$. C2 is determined to a $100\mu\text{F}$ aluminum electrolytic capacitor whose withstand voltage is 500V .

3.4. Design the Pulse Transformer TX1 [11]

(1) Establish the Turns Ratio n : The turns ratio determines the maximum voltage stress on the power transistor M5 in the absence of a leakage inductance spike. n can be calculated by the formula Equation (9).

$$n \approx U_{in}(\max) / U_{out}(\max) \quad (9)$$

Where, $U_{in}(\max)$ is the maximum input voltage 610V , and $U_{out}(\max)$ is the maximum output voltage 260V . Here, the result is $n = 2.5$.

(2) Check the Primary Inductance L_p and the Secondary Inductance L_s : The Flyback converter input power is $P_{in} = L_p I_{pm}^2 / (2T)$, output power is $P_{out} = C_2 [U_{out}(\max)^2 - U_{out}(\min)^2] / (2T)$, and they have the relation of $P_{out} = \eta P_{in}$. Primary peak current is $I_{pm} = V_{in} t_{on} / L_p$. So we can get the formula of L_p in Equation (10).

$$L_p = \frac{\eta V_{in}^2 t_{on}}{C_2 [U_{out}^2(\max) - U_{out}^2(\min)]} \quad (10)$$

Where, the V_{in} means the converter input voltage and $V_{in} = 600\text{V}$, turns ratio is $\eta = 0.9$, the maximum output voltage is $U_{out}(\max) = 260\text{V}$, the minimum output voltage is $U_{out}(\min) = 150\text{V}$, $C_2 = 100\mu\text{F}$. The "on" time $t_{on} = 5\mu\text{s}$. So the result of Equation (10) is $L_p = 179\text{mH}$.

(3) Check the Primary/Secondary Winding Turns N_p and N_s : To choose ferrite core with the saturation flux density $B_s = 0.35\text{T}$, $B_m = B_s/3$. The core effective cross-sectional area S_c and bobbin window area S_b meet the inequality Equation (11):

$$S_c S_b \geq \frac{P_o}{2jB_m f K_u \eta} \quad (11)$$

Where, the current density $j = 3\text{A/mm}^2$, $K_u = 0.3$, to choose GU36×22 tank-type core ($d_2 = 1.63\text{cm}$, $d_3 = 0.52\text{cm}$ and $S_c = 1.87\text{cm}^2$). The primary turns can be estimated as 69 by the

formula $N_p = L_p I_{pm} / S_c B_m$. The secondary turns can be estimated as 30 by the formula $N_s = N_p U_{out(max)} / U_{in}$.

(4) Check the Gap Length: The formula of gap length is shown in Equation (12):

$$l_g = \frac{100 \mu_r \mu_0 N_p^2 S_c}{L_p} \quad (12)$$

Where, the relative air permeability $\mu_r = 1$, vacuum permeability $\mu_0 = 4\pi \times 10^{-7} \text{H/m}$, primary turns $N_p = 69$, $L_p = 179 \text{mH}$, $S_c = 1.87 \times 10^{-4} \text{m}^2$, so the gap length is $l_g = 0.62 \text{mm}$.

3.5. Estimate the Switch M5

When the MOSFET is off the power switch has the biggest voltage stress $U_{in(max)} = 610 \text{V}$, so MOSFET's U_{ce0} can be chose as $2U_{in(max)} = 1220 \text{V}$. The maximum current of power switch is $I_{mp} = 2 \text{A}$. It's necessary two MOSFETs are connected in series in the circuit, and MOSFET *SPB17N80C3* ($V_{DSS} = 800 \text{V}$, $I_D = 17 \text{A}$) is selected as the switch M5.

4. Circuit Simulation

In the simulation, the transmitter circuit operating frequency is 25Hz, $U_{set} = 600 \text{V}$, $I_1 = 30 \text{A}$, $L_1 = 4.8 \text{mH}$, $R_1 = 3.5 \Omega$. The simulation software is PSpice (Version 16.5), and the simulation waveform is shown in Figura 4. In order to observe the waveform details, Figure 4 is partially unfolded, as shown in Figure 5. As seen in the C1 voltage waveform, $U_{C1}(t)$ rapidly increases from the bus voltage 150V to the setting value 600V in the first some launch cycles. Then it keeps at 600V, and only has a fluctuation of 8V (1.3%).

When the C1 voltage reaches 600V, the constant voltage circuit begins to work; the current begins to flow through transformer primary; control pulse appears in M5 gate; C2 begins to be charged and discharges periodically. As seen in L1 current waveform, the falling edge is linear and the turn-off delay is about 230 μs . The simulation verifies the correctness of theoretical derivation and circuit design.

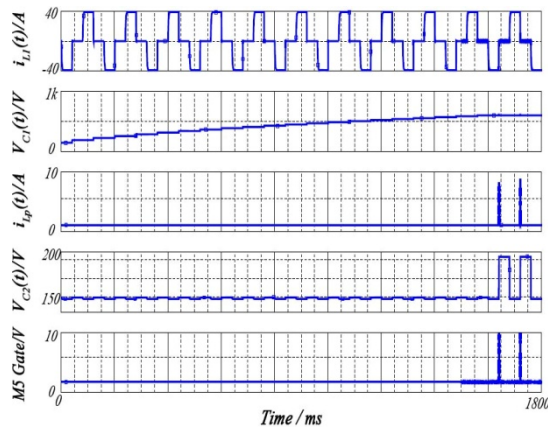


Figure 4. Flyback Circuit Simulations

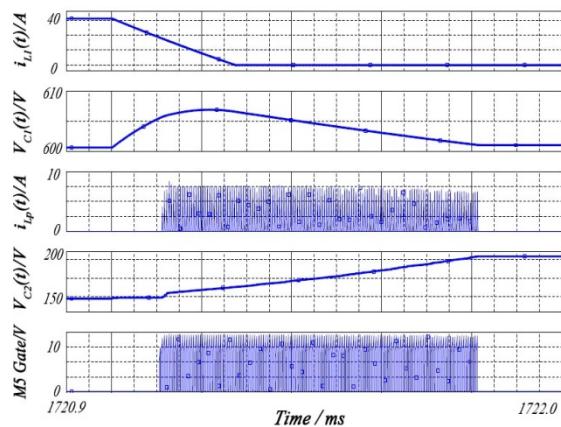


Figure 5. Current-off Period Simulations

5. Experiment

In the experiment, a 2000m cable is laid as a 500m \times 500m square transmittal coil. The current frequency is 25Hz and the current is 30A. Capacitor C1 is chose 100 μF aluminum electrolytic capacitors with a withstand voltage 1000V. Power transistor's model is *SPB17N80C3* ($V_{DSS} = 800 \text{V}$, $I_D = 17 \text{A}$). We pick LM319 with temperature range: $-40 \text{ }^\circ\text{C}$ to $+125 \text{ }^\circ\text{C}$ for the high speed comparators U1, U2. 200 kHz pulse generator V3 actually is realized by a 555 circuit. In the experiment, due to the performance of the DC power supply can not meets

the requirement of large inductive load, and the maximum transmittal current can only reaches 30A.

Due to the impact of a strong electromagnetic interference the oscilloscope waveform distorts when the transmittal current is 30A. Figure 6 and 7 show the experimental waveforms when the current is 25A. In the Figure 7, $i_L(t)$, $i_o(t)$ are measured by using the Hall current sensor and $U_{C2}(t)$, $U_{C1}(t)$ are measured with two oscilloscope voltage probes after being passed through a partial pressure circuit.

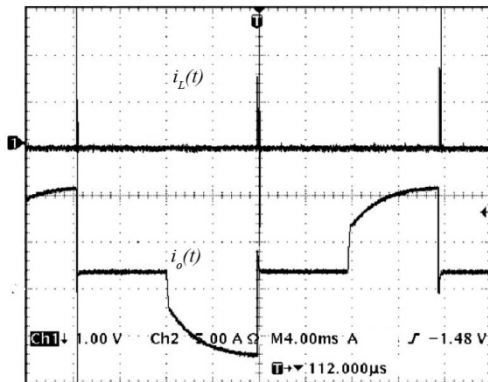


Figure 6. Waveforms of $i_L(t)$ and $i_o(t)$

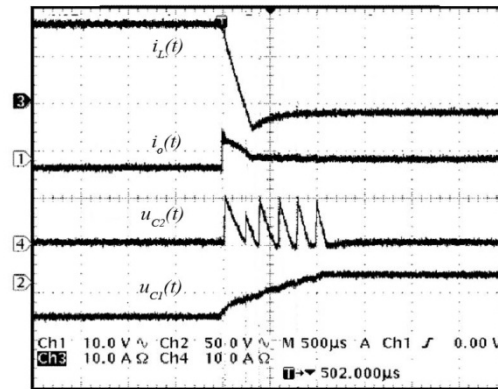


Figure 7 Details of $i_L(t)$, $i_o(t)$, $u_{C2}(t)$ and $u_{C1}(t)$ Waveforms during Current Falling

As we can see in the figures, the capacitor C1 voltage fluctuates between 598~609V and the fluctuation range less than 10V. Because the coil current decreases linearly, the function of constant voltage clamping has been achieved. Under the condition of 2000m transmittal coil, the turn-off delay is 250 μ s. From the rising edge of the transmittal current waveform view, the circuit achieves the function of energy feedback and the purpose of accelerating the forming of stable primary field.

The parasitic inductance, capacitance of power transistor, diode and external electromagnetic interference make little error between the experimental result and the simulation result. We can still come to the conclusion that the experimental result is basically consistent with the simulation result.

6. Conclusion

The paper presents a novel TEM transmitter using the Flyback topology fixed voltage clamping circuit. The circuit achieves a steep linear falling edge of the TEM pulse current by clamping the coil voltage during current falls with a fixed high voltage to meet the demand of the TEM geological exploration. The circuit is designed and optimized by MATLAB, simulated by the PSpice. Simulation and experiment proof the current falling edge has a high linearity and the turn-off delay significantly reduces. The new circuit has less power loss than the reported similar circuits, improves the rising edge of the coil current and achieves energy feedback. The Flyback topology fixed voltage clamping circuit is an excellent and practical pulse current supply circuit for the TEM transmitter.

Acknowledgments

This paper is supported by the National Natural Science Foundation of China (Grant No.61102115) and Natural Science Foundation of Guangxi (Grant No.2012GXNSFBA053177).

References

- [1] Du Mingming, Fu Zhihong, Zhou Luowei. A energy feedback fixed voltage clamp bipolar pulse current supply. *Transactions of China Electrotechnical Society*. 2007; 22(8): 57-62.
- [2] Luo Mingzhang. Research on pulsed electromagnetic method and the hardware implementation. Hubei: Yangtze University. 2012;6-12.
- [3] Cao Jian-zhang, Song Jian-ping, Tang Tian-tong. The experimental study of the absorption loop of the power MOSFET switch circuit. *Power Electronics Technology*. 1997; 31(4): 58-60.
- [4] Fu Zhihong, Zhou Luowei, Su Xiangfeng. *Two novel quasi-resonant current steep pulse shaping circuit*. Proceedings of the CSEE. 2006; 26(5): 70-75.
- [5] Ales Leban, Danijel Voncina. Pulse current source with high dynamic. EUROCON 2003, Computer as a Tool. The IEEE Region 8. 2003; 2(2):297-300.
- [6] Purwoharjono, Abdillah M, Penangsang O, etal. Optimal placement and sizing of thyristor-controlled series-capacitor using gravitational search algorithm. *TELKOMNIKA*. 2012; 10(5): 891-904.
- [7] P Turoskay, S Zach. *Deep earth detection by EM signals*. The 21st IEEE Convention of the Electrical and Electronic Engineers. Israel. 2000; 175-178.
- [8] Fu Zhihong. The special power of the electromagnetic detection technology. Chongqing: Chongqing University. 2007; 33-36.
- [9] Wu Zhonghua, Li Wenyao. The exact expression of the rectangular coil self-inductance. *Geophysical and Geochemical Exploration*. 2011; 33(5): 511-516.
- [10] Xinze Z, Meiyun Z, Wei P, etal. Analysis of contact characteristic of overhead line and suspension clamp. *TELKOMNIKA*. 2013; 11(3): 1456-1464.
- [11] Abraham Pressman. *Switching Power Supply Design*. Third edition. New York: McGraw-Hill. 2009; 117-184.